crystals

MDPI

Article

Novel Crystalline Salts of 4-Piperidyl- and 4-Pyridylmethylamines Prepared by Catalytic Hydrogenation of 4-Pyridinecarbonitrile: Crystallographic Unit Cells Based on Powder XRD Patterns by Using the *DASH* Program Package

János Madarász [1] and László Hegedűs [2,*]

[1] Department of Inorganic and Analytical Chemistry, Faculty of Chemical Technology and Biotechnology, Budapest University of Technology and Economics, Műegyetem rkp. 3, H-1111 Budapest, Hungary; madarasz.janos@vbk.bme.hu

[2] Department of Organic Chemistry and Technology, Faculty of Chemical Technology and Biotechnology Budapest University of Technology and Economics, Műegyetem rkp. 3, H-1111 Budapest, Hungary

* Correspondence: hegedus.laszlo@vbk.bme.hu; Tel.: +36-1-4631261

Abstract: Structures of some hydrogenated products and intermediates, prepared by a heterogeneous Pd/C or Ru/C catalyst starting from 4-pyridinecarbonitrile (**4PN**), in water and in the presence of an acidic additive (HCl or H_2SO_4), were confirmed in various salt forms of 4-piperidylmethylamine (**4PIPA**) and 4-pyridylmethylamine (**4PA**). Crystallographic unit cell structure of the completely hydrogenated product salts (**4PIPA·H_2SO_4** and **4PIPA·2HCl**) showed a common double-protonated **[4PIPA+2H]$^{2+}$** divalent cation structure, also proved by FT-IR, and that of the **4PA·H_2SO_4** intermediate salt was also indexed and modeled by means of powder X-ray diffraction, applying the *DASH* 4.0 software package and crystal coordinates coming from former single-crystal X-ray structure determination. Formations of the anhydrous and hydrated forms of **4PA·0.5H_2SO_4·xH_2O** (x = 0 or x = 0.5, hemisulfates) were also studied by powder XRD and FT-IR spectroscopy for comparing these crystal structures.

Keywords: 4-piperidylmethylamine; 4-pyridylmethylamine; sulfate salt; powder X-ray diffraction; indexing

Citation: Madarász, J.; Hegedűs, L. Novel Crystalline Salts of 4-Piperidyl- and 4-Pyridylmethylamines Prepared by Catalytic Hydrogenation of 4-Pyridinecarbonitrile: Crystallographic Unit Cells Based on Powder XRD Patterns by Using the *DASH* Program Package. *Crystals* **2024**, *14*, 938. https://doi.org/10.3390/cryst14110938

Academic Editor: Kaveh Edalati

Received: 28 September 2024
Revised: 15 October 2024
Accepted: 24 October 2024
Published: 29 October 2024

1. Introduction

Aminomethyl-substituted pyridine and piperidine constitutional isomers can be synthesized by liquid-phase heterogeneous catalytic hydrogenation of the corresponding pyridinecarbonitriles using a 10% Pd/C catalyst [1]. Both the partially hydrogenated pyridylmethylamines and the completely saturated piperidylmethylamines can be obtained and captured in strongly acidic aqueous medium as hydrochloride or sulfate salts (Figure 1).

These *N*-heterocyclic compounds are valuable raw materials and intermediates for the preparation of pharmaceuticals, agricultural chemicals, or other products. Piperidines especially have a wide range of biological effects, including analgesic, antihypertensive, central nervous system depressant, antibacterial, or antifungal activities. For example, a novel class of potent and highly selective M_3 muscarinic antagonists [2] or human β_3 adrenoreceptor agonists [3,4] containing 4-piperydylmethylamine pharmacophore have been published recently. Furthermore, new phase-shifting 2-, 3-, or 4-pyridylmethylamine-based solvents with high CO_2 capture capacity (11−20 wt%) were reported, which readily bind CO_2 to form a crystalline salt under both dry and wet conditions [5]. In addition, the active pharmaceutical ingredients (APIs) are often produced and marketed in crystalline forms (e.g., hydrochlorides, sulfates, formates, etc.), therefore revealing their structures are important in both scientific and technological aspects.

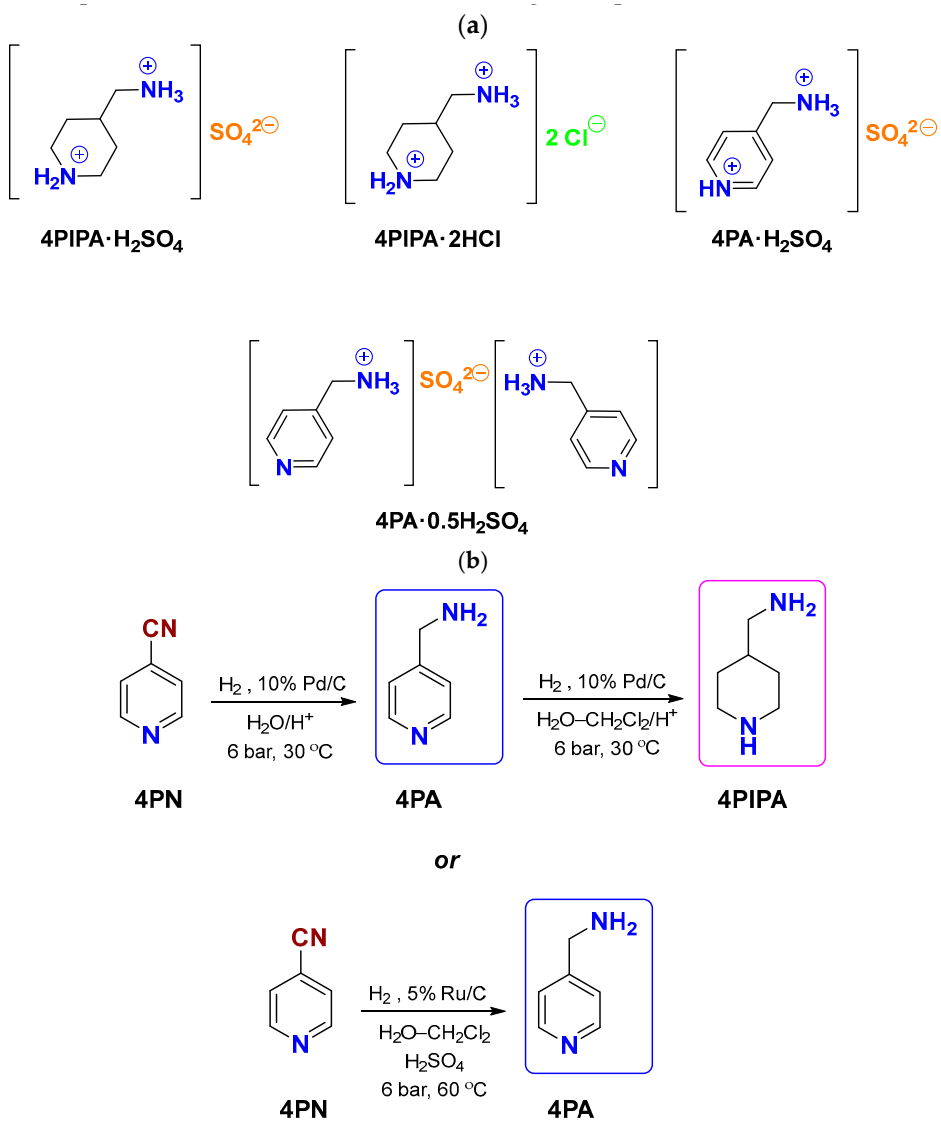

Figure 1. (**a**) The 2D structures of 4-piperidyl- (**4PIPA**) and 4-pyridylmethylamine (**4PA**) sulfate and hydrochloride salts; (**b**) hydrogenation of 4-pyridinecarbonitrile (**4PN**) to **4PIPA** or **4PA** over a 10% Pd/C or a 5% Ru/C catalyst.

In some cases, the solid-state structures of these crystalline salts are already known, and the product salts can also be identified by their powder X-ray diffraction pattern, generated from their atomic coordinates obtained from former single-crystal structure determinations. Checking for similar salts in the single-crystal structural database (CSD) [6], it can be observed that the various aminomethyl-substituted pyridine isomer salts may occur in either single- or double-protonated forms. As sulfate salts, double-protonated monosulfate–monohydrate ones were reported for 2- and 3-pyridylmethylamines under CSD codes LAQQEB [7] and ATUXUJ [8], respectively, while as hydrochloride salts, 2- and 3-pyridylmethylamine dihydrochlorides, under CSD codes PEKCIS [9] and PICAMC01 [10], were also published. Whereas, there are both mono- [11] and dihydrochloride [12] salts of 4-pyridylmethylamine in the CSD, with solved and known single-crystal structures (under CSD codes QANWOS and IGHUU) containing single- and double-protonated cations, respectively.

Among the corresponding piperidylmethylamine salts, whose structures are rather rarely found in the CSD, only that of 4-piperidylmethylamine diperchlorate is solved as a single crystal with a diprotonated cation, but with two modifications under CSD codes VIVLEU and VIVLEU01 [13]. The (*R*)- and (*S*)-2-piperidylmethylamine dihydrochloride

salts are also known, and the single-crystal atomic coordinates are available for the (*R*)-enantiomer under CSD code XOMMAO [14].

To our best knowledge, the structures of these 4-piperidyl- and 4-pyridylmethylamine salts prepared by us have never been described in the literature; thus, we report the FT-IR spectra and crystallographic unit cells of **4PIPA·H_2SO_4**, **4PIPA·2HCl**, **4PA·H_2SO_4**, and **4PA·0.5H_2SO_4** salts obtained by the *DASH* 4.0 software package [15] based on their powder XRD patterns. This program tool is a versatile, graphical, user interface-driven computer program that was distributed earlier within the Cambridge Structural Database System package [6], but now, it is available separately and as an open source [16]. Among others, it was originally planned to be used for the structure solution [17–20] from powder XRD data collected in high resolution by synchrotron radiation, especially to determine the crystal structures of large-volume commercial pharmaceuticals [21,22]. However, it could be useful for the structural evaluation of powder diffraction data collected by laboratory X-ray tubes as well [23,24].

This work is part of a systematic investigation concerning the favorable cases using the *DASH* 4.0 program package for the extraction of any approximate but structural information from powder X-ray patterns of crystalline materials. Our purpose was also to find and demonstrate several cases, especially hydrochloride and sulfate salts that contain Cl or S as heavy elements, when reliable conjectures for crystallographic unit cells (parameters and a choice of reasonable space group) and the successful modeling of unit cell contents could be achieved, starting from the corresponding XRD patterns measured by a common laboratory technique. Naturally, the reliability of these trials is lower than that of single-crystal structural determinations, but it could be useful when single crystals are not available at all.

2. Materials and Methods

2.1. Materials

The samples of **4PIPA·H_2SO_4**, **4PIPA·2HCl**, and **4PA·0.5H_2SO_4** were prepared according to our published Pd-catalyzed hydrogenation method [1], while that of **4PA·H_2SO_4** was synthesized by using our modified process, in which a 5% Ru/C catalyst was applied under very similar conditions (catalyst/substrate ratio = 0.2 g·g^{-1}, H_2SO_4/**4PN** molar ratio = 1.0, water/dichloromethane, 60 °C, 6 bar, reaction time: 7 h). Their chemical compositions were analyzed by GC–MS, as well as ^{1}H and ^{13}C NMR measurements in their free base form, prepared just prior to the analyses. Their spectroscopic data were the following: **4PIPA·H_2SO_4** mp. 285–287 °C (decomp.); **4PIPA·2HCl** mp. 293–298 °C (decomp.); **4PA·0.5H_2SO_4** mp. 162–168 °C (decomp.); **4PA·H_2SO_4** mp. 144–146 °C (decomp.); **4PIPA** GC–MS *m*/*z* (rel%) 114(27), 96(20), 84(39), 69(32), 56(100); ^{1}H NMR ($CDCl_3$, 500 MHz) δ ppm 1.38–1.53 (m, 5H, CH_2CHCH_2), 2.35 (br s, 3H, NH and NH_2), 2.94 (d, *J* = 5.0 Hz, 2H, CH_2NH_2), 3.40–3.47 (m, 4H, CH_2NHCH_2); ^{13}C NMR ($CDCl_3$, 125 MHz) δ ppm 25.7 (CH_2CHCH_2), 31.6 (CH_2CHCH_2), 43.4 (CH_2NHCH_2), 43.7 (CH_2NH_2). **4PA** GC–MS *m*/*z* (rel%) 108(12), 107(28), 80(100), 51(13); ^{1}H NMR ($CDCl_3$, 500 MHz) δ ppm 1.79 (br s, 2H, NH_2), 3.88 (s, 2H, CH_2NH_2), 7.24 (d, *J* = 5.0 Hz, 2H, Pyr-*CH*CCH), 8.52 (d, *J* = 5.0 Hz, 2H, Pyr-*CH*NCH); ^{13}C NMR ($CDCl_3$, 125 MHz) δ ppm 45.4 (CH_2NH_2), 122.0 (Pyr-*CH*CCH), 149.8 (Pyr-*CH*NCH), 151.9 (Pyr-CHCCH).

2.2. Characterization Methods

2.2.1. Powder X-Ray Diffraction (XRD)

Powder XRD patterns were recorded with an X'pert Pro MPD (Malvern Panalytical, Malvern, UK) multipurpose X-ray diffractometer using Cu-Kα radiation (λ = 1.5406 Å), with Ni foil as a β-filter, an X'celerator detector, and "zero background" single-crystal silicon or "top-loaded" sample holders in the range of 2θ = 4–52°. The X-ray tube was operating at 40 kV and 30 mA. For purposes of indexing the crystallographic unit cell [25], searching for space group symmetries [26,27], and structural modeling with simulated annealing, originally built-in or invocable program routines of the *DASH* 4.0 software package [15] and a measuring step size of 0.0167° up to 2θ = 52° were applied.

2.2.2. FT-IR Spectroscopy

Fourier transform infrared (FT-IR) spectra of the solid powder samples were measured by the PE System 2000 (PerkinElmer, Waltham, MA, USA) FT-IR spectrophotometer in a KBr pastille, between 500 and 4000 cm^{-1}, at a resolution of 4 cm^{-1}.

3. Results and Discussion

3.1. FT-IR Investigations

3.1.1. Comparison of the Completely Hydrogenated **4PIPA·H_2SO_4** and **4PIPA·2HCl** Product Salts

FT-IR spectra of the two 4-piperidylmethylamine (**4PIPA**) products isolated in the form of a hydrochloride or sulfate salt are shown in Figure 2. As seen, they were very similar to each other, except the two strong absorption bands peaked at 1125 and 620 cm^{-1}. Their highly related FT-IR spectral features can be explained by their analogous saltlike structures. This high similarity is most probably due to their common organic cations, while their differences can be elucidated by the diverse vibration opportunities of their different anions (chloride and sulfate, respectively). The completely hydrogenated **4PIPA·H_2SO_4** and **4PIPA·2HCl** product salts should have the same type of cation, most probably a double-protonated one on the nitrogen of both the pyridine ring and the methylamine part. It was obvious that the simple chloride counterion had no absorption bands, while the sulfate anion showed two strong IR-active stretching vibration bands (ν_3 and ν_4) at around 1125 and 620 cm^{-1} [24]. It can clearly be observed that the common **[4PIPA+2H]$^{2+}$** divalent cations took part in the same types of hydrogen bonding systems in both salts, resulting in almost identically sophisticated, broadened, and similarly extended absorption band systems exhibited between 1900 and 3700 cm^{-1}.

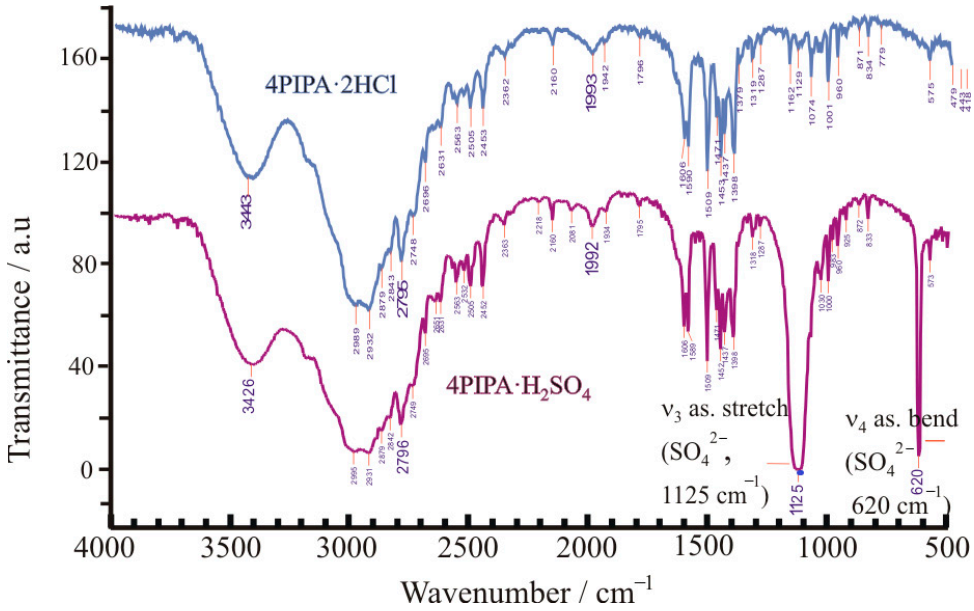

Figure 2. FT-IR spectra of the fully hydrogenated **4PIPA·2HCl** (top) and **4PIPA·H_2SO_4** (bottom) product salts.

3.1.2. Comparison of the Partially Hydrogenated **4PA·0.5H_2SO_4·xH_2O** (x = 0 or x = 0.5) and **4PA·H_2SO_4** Product Salts

FT-IR spectra of the two 4-pyridylmethylamine products isolated in the forms of their hemisulfate and monosulfate salts are shown in Figure 3. These spectra had no similarities, except the two strong absorption bands that peaked at around 1118–1120 and 619–620 cm^{-1}, which came from the common inorganic sulfate anion [28]. The highly different FT-IR spectral features of these sulfate salts can be explained by their diverse saltlike structures, containing one and two protonated *N*-containing groups in the hemi- and monosulfate,

respectively. These spectral differences indicate that the 4-pyridylmethylamine (**4PA**) was only protonated to the methylammonium cation in the case of hemisulfate, while it was protonated to pyridinium- and ammonium-type divalent cations in the case of monosulfate salt. The diverse absorption band structures occurred both in the fingerprint regions and in the wide hydrogen bonding regions. The different degrees of protonation of pyridine parts can also be responsible for the various aromatic ring vibration modes/bands of the obtained mono- and divalent cations observed in the range of 1580–1650 cm^{-1}. However, the variable degree of hydration of the hemisulfate salt (**4PA·0.5H$_2$SO$_4$·xH$_2$O**) resulted in two different XRD patterns for the anhydrous (x = 0) and the hemihydrate (x = 0.5) forms (Section 3.2.2.), but this did not significantly affect the measured IR spectra (Figure 4).

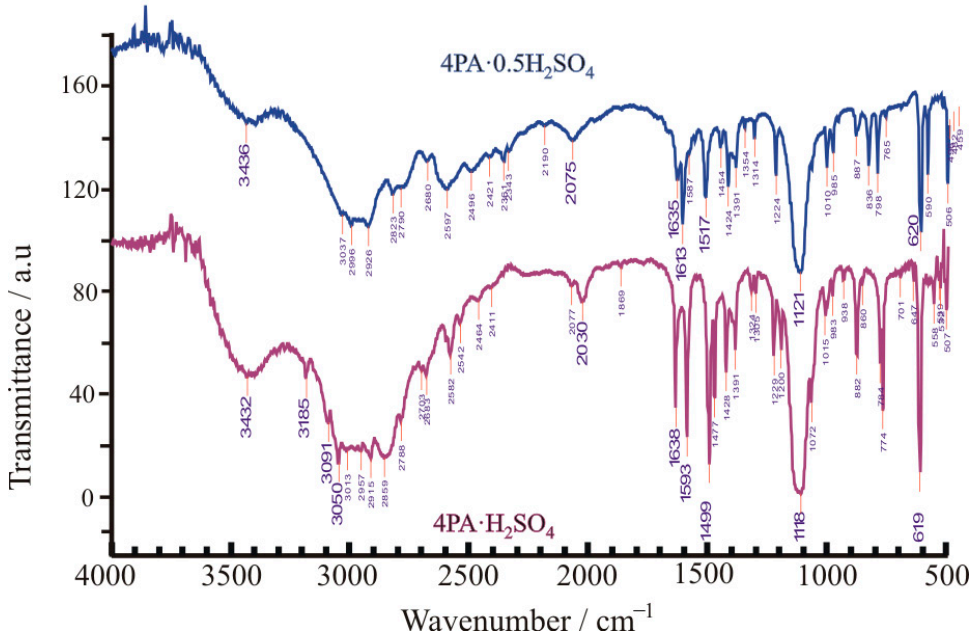

Figure 3. FT-IR spectra of partially hydrogenated **4PA·0.5H$_2$SO$_4$**·(top) and **4PA·H$_2$SO$_4$** (bottom) product salts.

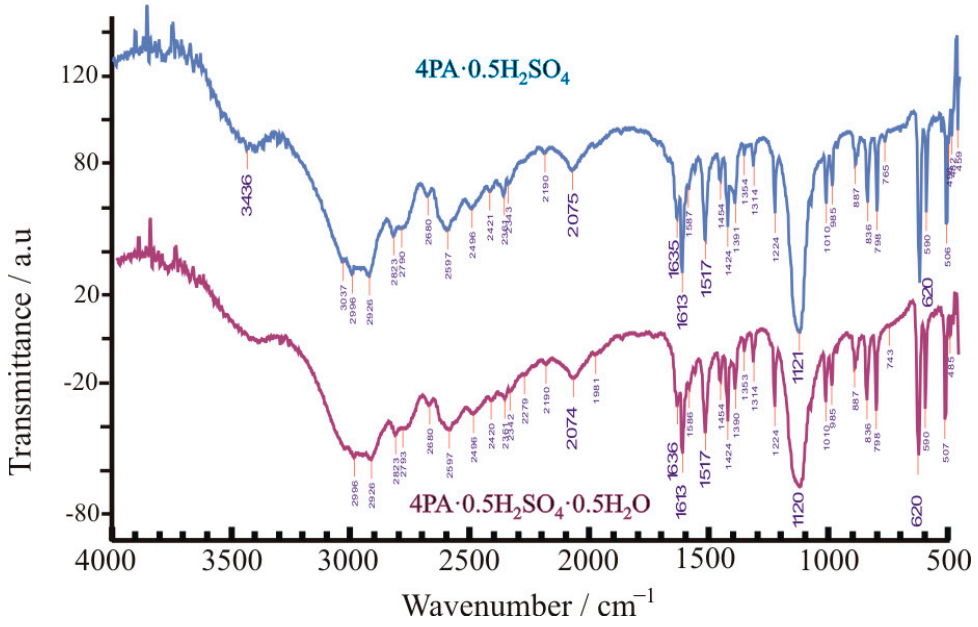

Figure 4. FT-IR spectra of partially hydrogenated **4PA·0.5H$_2$SO$_4$** (top) and **4PA·0.5H$_2$SO$_4$·0.5H$_2$O** (bottom) product salts.

3.2. Powder X-Ray Diffraction Examinations

3.2.1. Estimation and Modeling of the Crystallographic Unit Cells of **4PIPA·H_2SO_4** and **4PIPA·2HCl** Product Salts

Both the final product samples of **4PIPA·2HCl** and **4PIPA·H_2SO_4**, as prepared, were found to be crystalline ones by powder X-ray diffraction (Figure 5a,b). Their XRD patterns were subjected to powder pattern indexing, also known as *Dicvol* [25], using the interactive *DASH* 4.0 program package [15]. In both cases, the indexing algorithms led to definite unit cell parameters of reasonable volume of the crystallographic cell and appropriate cell symmetry. For **4PIPA·2HCl,** an orthorhombic space group, s.g. No. 61 (*Pcab*), while for **4PIPA·H_2SO_4,** a triclinic space group, s.g. No. 2 (*P-1*), were found to be the proper ones. In addition, a built-in *ExtSym* (*Extinction Symbol*) program subroutine [26,27], which is an algorithm for helping to choose the extinction symbol/space group based on probability levels, was also used during the indexing procedure. The proposed cell parameters are summarized in Table 1.

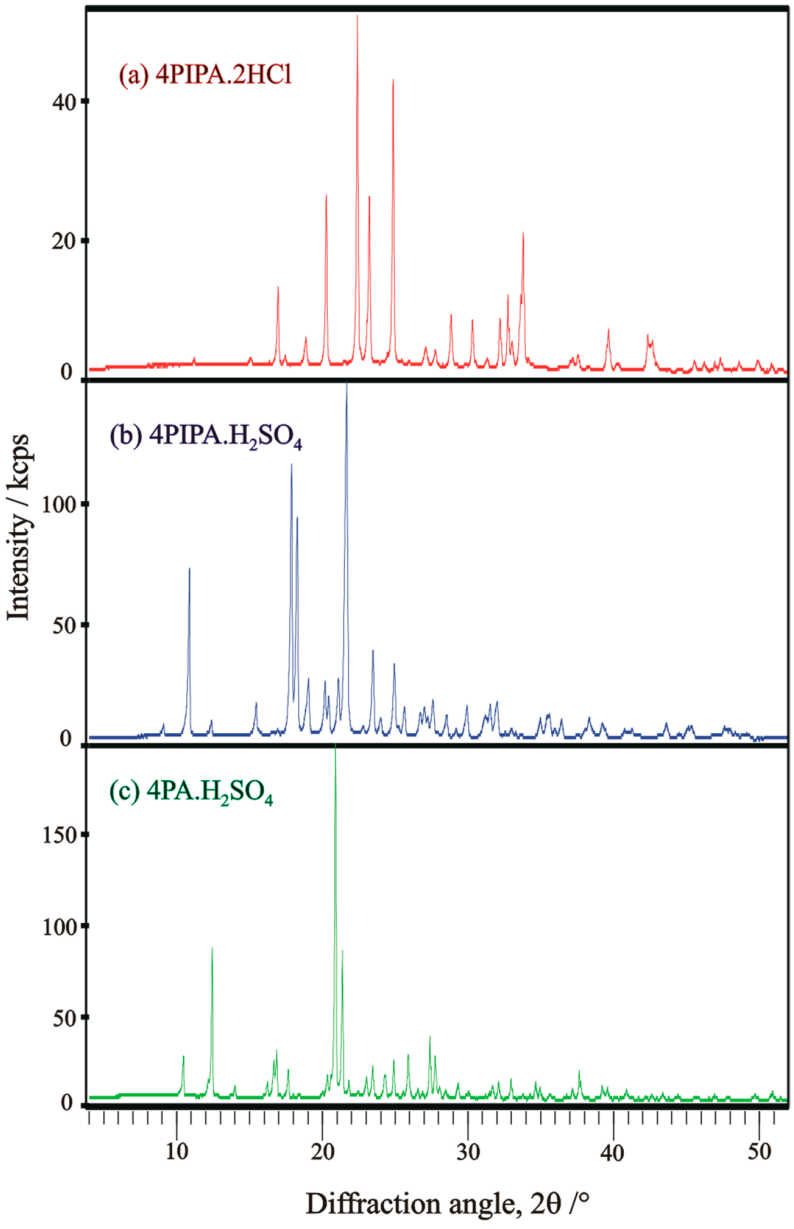

Figure 5. XRD patterns of **4PIPA·2HCl** (**a**), **4PIPA·H_2SO_4** (**b**), and **4PA·H_2SO_4** (**c**) product salts.

Table 1. Crystallographic unit cell parameters for crystalline **4PIPA·2HCl** and **4PIPA·H_2SO_4** salts obtained from their powder XRD patterns [a].

Salt Samples/Formula Unit **Features of Crystallographic Unit Cells**	**4PIPA ·2HCl** **4-Piperidiniummethyl-ammonium Dichloride** **$C_6H_{14}N_2$·2HCl =** **$C_6H_{16}N_2^{2+}$ $2Cl^-$**	**4PIPA·H_2SO_4** **4-Piperidiniummethyl-ammonium Monosulfate** **$C_6H_{14}N_2$·H_2SO_4 =** **$C_6H_{16}N_2^{2+}$ SO_4^{2-}**
Crystal system	orthorhombic	triclinic
Space group (s.g. No.)	*Pcab* (No. 61)	*P*-1 (No. 2)
a (Å)	17.601	10.431
b (Å)	15.936	8.405
c (Å)	7.188	5.978
α (°)	90	86.70
β (°)	90	106.40
γ (°)	90	104.24
V (Å^3)	2016.06	487.30
Z/*Z*′ (–)	8/1	2/1
V_m (Å^3)	252.01	243.65
Merit of Pawley refinement fitting (χ^2)	26.98	22.2
Estimated zero-point shift (°)	0.0898	0.0378

[a] Estimated uncertainty of unit cell parameters is 0.005 Å and 0.03°.

A structural skeleton for the diprotonated cation (**[4PIPA+2H]$^{2+}$**) was borrowed from the formerly solved 4-piperidylmethylamine diperchlorate salt structure (under CSD code VIVLEU [13], room temperature modification), with known bond distances and angles. In both cases, it could be applied as a structural model for further simulations on the variation of the single torsion angle of the cation and the positions of anions using simulated annealing randomization and a final *Simplex* algorithm built in the *DASH* 4.0 program package.

In case of the **4PIPA·2HCl** = **[4PIPA+2H]$^{2+}$ $2Cl^-$** salt, the received orthorhombic space group, s.g. No. 61 (*Pcab*), with the *Z* = 8 formula unit per unit cell volume of 2016.0 Å^3 (*Z*′ = 1 formula unit per asymmetric unit of 252.0 Å^3) seemed to be its valid crystallographic unit cell and space group choice, as the structural modeling process in all trials, applying the mentioned room temperature dication structure, led to quite a reasonable arrangement of both cations and anions, where the protonated primary ammonium group was involved in three hydrogen bonds with three chloride anions, while the secondary one was involved in two hydrogen bonds with two chloride anions (Figure 6a). One of the chloride anions had two hydrogen-bridged connections, while the other one had three ones to nitrogen atoms of neighboring dications (**[4PIPA+2H]$^{2+}$**), without any voids in the formed lattice (Figure 6b). Since each modeling trial was ended in a significant *Simplex* optimization, almost the same structural feature/picture was achieved.

In case of the **4PIPA·H_2SO_4** = **[4PIPA+2H]$^{2+}$$SO_4^{2-}$** salt, the obtained triclinic space group, s.g. No. 2 (*P*-1), with a *Z* = 2 formula unit per unit cell volume of 487.3 Å^3 (*Z*′ = 1 formula unit per asymmetric unit of 243.65 Å^3) seemed to be quite the valid crystallographic unit cell and space group choice because the structural modeling process in most of the trials, applying the abovementioned room temperature dication structure, led to quite a reasonable arrangement of cations and anions. It meant that the protonated primary ammonium group was involved in four hydrogen bonds (one hydrogen in a bifurcated way, as well), while the secondary one was involved in two hydrogen bonds with oxygen atoms of two sulfate anions (Figure 7a). Each sulfate anion had six hydrogen-bridged connections to nitrogen atoms of five neighboring dications (**[4PIPA+2H]$^{2+}$**), without any voids in the formed lattice (Figure 7a,b).

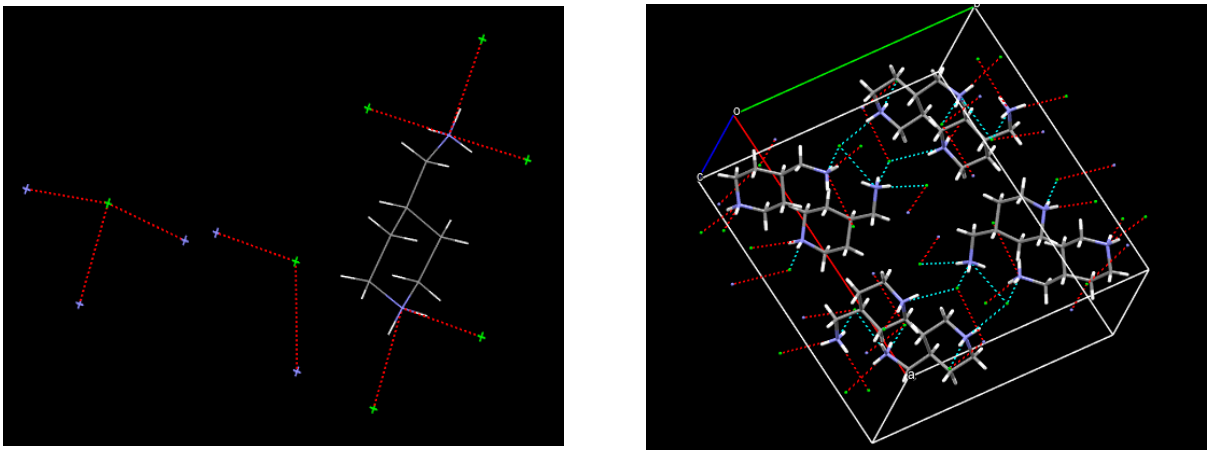

(**a**) (**b**)

Figure 6. Hydrogen bonding opportunities (**a**) and arrangements of ions without voids (**b**) in the proposed unit cell structure of **4PIPA·2HCl** = **[4PIPA+2H]$^{2+}$ 2Cl^{-}** salt.

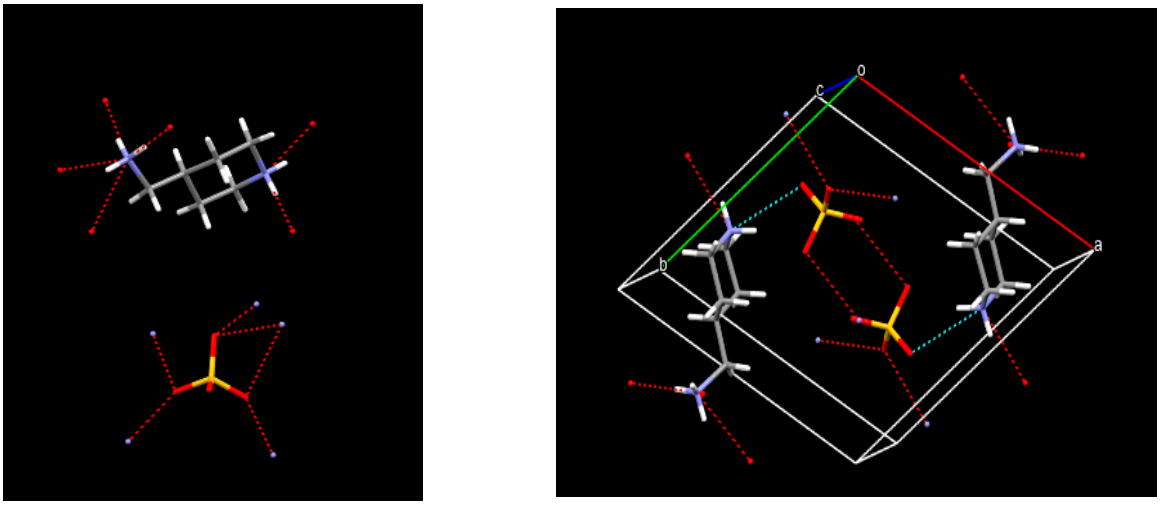

(**a**) (**b**)

Figure 7. Hydrogen bonding opportunities (**a**) and arrangements of ions without voids (**b**) in the proposed unit cell structure of **4PIPA·H_2SO_4** = **[4PIPA+2H]$^{2+}$ SO_4^{2-}** salt.

3.2.2. Estimation of the Crystallographic Unit Cell of **4PA·0.5H_2SO_4·xH_2O** (x = 0.5 or x = 0) Intermediate Salts

The synthesized pyridyl hemisulfate intermediate (**4PA·0.5H_2SO_4·xH_2O**) samples were obtained in hemihydrate form (x = 0.5), but after a longer period of aging (1–1.5 years), they turned into the anhydrous (x = 0) form and exhibited different XRD patterns (Figure 8a,b). This latter one was also confirmed by a thermal treatment of the fresh hemihydrate sample (**4PA·0.5H_2SO_4·0.5H_2O**) at 120 °C (Figure 8c). All of them were also subjected to powder pattern indexing by *Dicvol* [25] using the interactive *DASH* 4.0 program [15]. The pattern of fresh, hydrated hemisulfate (**4PA·0.5H_2SO_4·0.5H_2O**) could be indexed in the monoclinic crystal system, and a space group, $P2_1/n$ (s.g. No. 14), was found to be an appropriate choice. For its aged and anhydrous form (**4PA·0.5H_2SO_4**), a triclinic crystal system with the *P*-1 (No. 2) space group was determined by using the built-in *ExtSym* algorithm [27]. The proposed cell parameters are summarized in Table 2. It has to be noted that no intermediate compounds were found; only physical mixtures of the hemihydrated and anhydrous forms were observed.

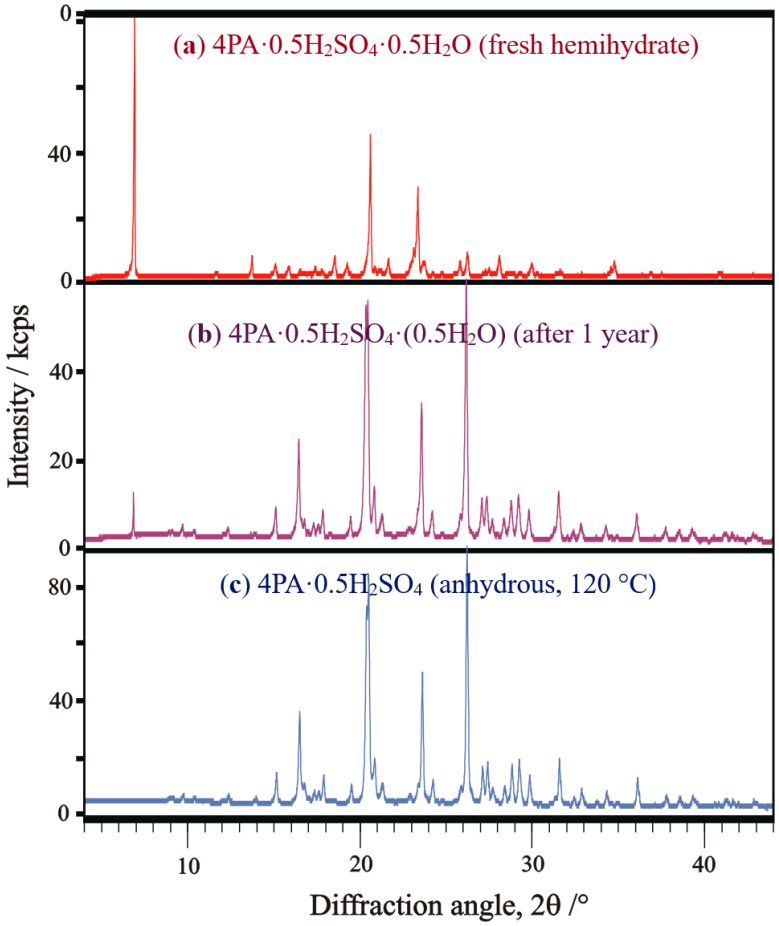

Figure 8. XRD patterns of the fresh (**a**), aged-for-1-year (**b**), and anhydrous (**c**) forms of crystalline **4PA·0.5H$_2$SO$_4$·xH$_2$O** (x = 0.5 or x = 0) hemisulfate salts.

Table 2. Proposed crystallographic unit cell parameters of hydrated and anhydrous forms of crystalline **4PA·0.5H$_2$SO$_4$·xH$_2$O** (x = 0.5 or x = 0) hemisulfate salts obtained from the measured powder XRD patterns [a].

Salt Samples/Formula Unit	**4PA·0.5H$_2$SO$_4$·0.5H$_2$O (Fresh, Hydrated) 4-Pyridylmethyl-ammonium Hemisulfate Hemihydrate**	**4PA·0.5H$_2$SO$_4$ (Aged, Anhydrous) 4-Pyridylmethyl-ammonium Hemisulfate**
Features of Crystallographic Unit Cell	**C$_6$H$_8$N$_2$·0.5H$_2$SO$_4$·0.5H$_2$O**	**C$_6$H$_8$N$_2$·0.5H$_2$SO$_4$**
Crystal system	monoclinic	triclinic
Space group (s.g. No.)	$P2_1/n$ (No. 14)	P-1 (No. 2)
a (Å)	17.194	10.273
b (Å)	5.874	11.403
c (Å)	15.393	16.134
α (°)	90	53.65
β (°)	101.43	107.86
γ (°)	90	106.71
V (Å^3)	1523.83	1434.96
Z/Z′ (–)	8/2	8/4
V_m (Å^3)	190.48	179.37
Merit of Pawley refinement fitting (χ^2)	234	80.4
Estimated zero-point shift (°)	–0.1238	–0.067

[a] Estimated uncertainty of unit cell parameters is 0.005 Å and 0.03°.

3.2.3. Estimation and Modeling of the Crystallographic Unit Cell of **4PA·H_2SO_4** Intermediate Salt

The intermediate pyridyl monosulfate sample of **4PA·H_2SO_4**, as obtained, was found to be crystalline using powder X-ray diffraction (Figure 5c). Its XRD pattern was also subjected to powder pattern indexing by *Dicvol* [25] and *McMaille* [29] methods using the interactive *DASH* 4.0 program package [15]. At the beginning, neither of the indexing algorithms led to definite unit cell parameters without an assumption of the reasonably high volume (about 1900 Å^3) of the crystallographic cell and an appropriate cell symmetry. Therefore, some indications were gathered about the related constitutional isomer pyridylmethylamine sulfate salts, where the double-protonated monosulfate–monohydrate salt of 2- and 3-(aminomethyl)pyridine (LAQQEB [7] and ATUXUJ [8]) had Z' = 223 and 221 Å^3 values, respectively. Using a rough estimation of volume per formula unit, assuming general density, it resulted in approx. 251 Å^3 [30]. Finally, the **4PA·H_2SO_4** salt could be indexed in an orthorhombic crystal system, and a space group, s.g. No. 61 (*Pbca*), was found to be an appropriate choice by applying the built-in *ExtSym* algorithm [27]. The proposed cell parameters are shown in Table 3.

Table 3. Crystallographic unit cell parameters for crystalline **4PA·H_2SO_4** salt obtained from the measured powder XRD patterns [a].

Salt Samples/Formula Unit **Features of Crystallographic Unit Cell**	**4PA·H_2SO_4** **4-Pyridylmethyl-ammonium Monosulfate** **$C_6H_8N_2·H_2SO_4 = C_6H_{10}N_2^{2+}\ SO_4^{2-}$**
Crystal system	orthorhombic
Space group (s.g. No.)	*Pbca* (No. 61)
a (Å)	17.101
b (Å)	14.372
c (Å)	7.819
α (°)	90
β (°)	90
γ (°)	90
V (Å^3)	1921.64
Z/Z' (–)	8/1
V_m (Å^3)	240.21
Merit of Pawley refinement fitting (χ^2)	44.65
Estimated zero-point shift (°)	0.144

[a] Estimated uncertainty of unit cell parameters is 0.005 Å and 0.03°.

Thus, in case of the **4PA·H_2SO_4** = **$[4PA+2H]^{2+}·SO_4^{2-}$** salt, the obtained orthorhombic space group, s.g. No. 61 (*Pbca*), with a Z = 8 formula unit per unit cell volume of 1921.6 Å^3 (Z' = 1 formula unit per asymmetric unit of 240.2 Å^3) seemed to be quite a valid crystallographic unit cell and space group choice. Since the structural modeling process, applying a former room-temperature dication structure (under CSD code IGAHUU [12]) led to a quite reasonable arrangement of cations and anions, where both the protonated primary and secondary ammonium groups of the dication were involved in hydrogen bonding with one oxygen atom of two separate sulfate anions (Figure 9). Each sulfate anion had two hydrogen-bridged connections to nitrogen atoms of two neighboring dications (**$[4PA+2H]^{2+}$**), without any voids in the formed lattice.

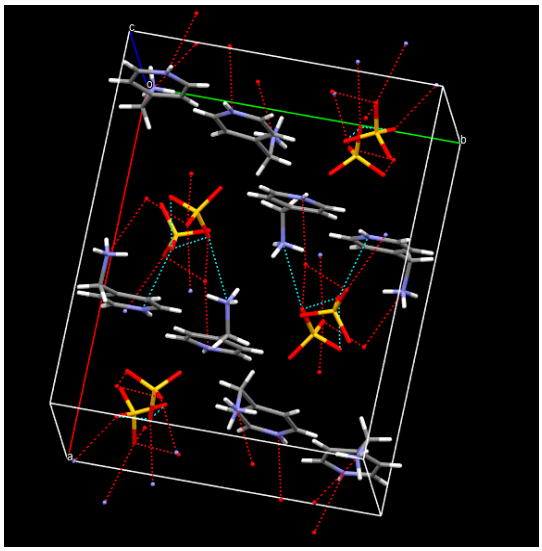

Figure 9. Hydrogen bonding opportunity arrangements of ions without voids in the proposed unit cell structure of **4PA·H_2SO_4** = **[4PA+2H]$^{2+}$·SO_4^{2-}** salt.

4. Conclusions

Structures of *N*-heterocylic amines (products and intermediates) prepared by heterogeneous catalytic hydrogenations over a Pd/C or Ru/C catalyst, starting from 4-pyridinecarbonitrile, in an aqueous acidic (HCl or H_2SO_4) medium were also confirmed to be 4-piperidylmethylamine (**4PIPA**) and 4-pyridylmethylamine (**4PA**) in crystalline forms of their novel salts by powder X-ray diffraction (XRD) structure predictions.

Crystallographic unit cell structure of the completely hydrogenated **4PIPA·2HCl** and **4PIPA·H_2SO_4** product salts containing the same double-protonated **[4PIPA+2H]$^{2+}$** divalent cation, whose presence was proved by FT-IR spectroscopy, and that of **4PA·H_2SO_4** intermediate salt were definitely indexed and modeled based on their powder X-ray diffraction profiles, applying both the tools of the *DASH* 4.0 software package and atomic coordinates taken from former single-crystal X-ray structure determinations of related compounds.

Formations of both the anhydrous and hydrated forms of 4-pyridylmethylamine hemisulfate (**4PA·0.5H_2SO_4·xH_2O**, x = 0 or x = 0.5) were also studied by powder XRD and FT-IR spectroscopy. It was found that the fresh, hydrated hemisulfate (**4PA·0.5H_2SO_4·0.5H_2O**) had a different crystal system (monoclinic) than that of the anhydrous form (**4PA·0.5H_2SO_4**, triclinic), i.e., a spontaneous transformation took place, resulting in diverse crystalline forms of this 4-pyridylmethylamine salt.

It was demonstrated that in some favorable cases, such as hydrochloride and sulfate salts, reliable conjectures for crystallographic unit cell parameters and modeling the unit cell contents could be achieved starting from the corresponding XRD patterns measured using a common laboratory technique and by using the *DASH* 4.0 program package. Obviously, the reliability of this method is lower than that of single-crystal structural determinations, but it could be a useful one when single crystals are not available at all.

Further investigations to propose the different salt structures of other *N*-heterocyclic amino compounds are in progress.

Author Contributions: Conceptualization, J.M. and L.H.; methodology, J.M; software, J.M.; validation, J.M. and L.H.; formal analysis, J.M.; investigation, J.M. and L.H.; writing—original draft preparation, J.M. and L.H.; writing—review and editing, J.M. and L.H.; visualization, J.M. and L.H.; supervision, L.H.; project administration, L.H.; funding acquisition, L.H. All authors have read and agreed to the published version of the manuscript.

Funding: This research was funded by The National Research, Development, and Innovation Office (NKFIH, Hungary). Project no. RRF-2.3.1-21-2022-00015 (PharmaLab) has been implemented with the support provided by the European Union.

Data Availability Statement: All the relevant data are included in this published article.

Acknowledgments: The authors are grateful to Krisztina Lévay and Cao Quynh An for their assistance in the preparation of these sulfate/hydrochloride salts.

Conflicts of Interest: The authors declare no conflicts of interest.

References

1. Lévay, K.; Madarász, J.; Hegedűs, L. Tuning the chemoselectivity of the Pd-catalysed hydrogenation of pyridinecarbonitriles: An efficient and simple method for preparing pyridyl- or piperidylmethylamines. *Catal. Sci. Technol.* **2022**, *12*, 2634–2648. [CrossRef]
2. Sagara, Y.; Sagara, T.; Uchiyama, M.; Otsuki, S.; Kimura, T.; Fujikawa, T.; Noguchi, K.; Ohtake, N. Identification of a Novel 4-Aminomethylpiperidine Class of M_3 Muscarinic Receptor Antagonists and Structural Insight into Their M_3 Selectivity. *J. Med. Chem.* **2006**, *49*, 5653–5663. [CrossRef] [PubMed]
3. Steffan, R.J.; Ashwell, M.A.; Solvibile, W.R.; Matelan, E.; Largis, E.; Han, S.; Tillet, J.; Mulvey, R. Novel Substituted 4-Aminomethylpiperidines as Potent and Selective Human β_3-Agonists. Part 1: Aryloxypropanolaminomethylpiperidines. *Bioorg. Med. Chem. Lett.* **2002**, *12*, 2957–2961. [CrossRef]
4. Steffan, R.J.; Ashwell, M.A.; Solvibile, W.R.; Matelan, E.; Largis, E.; Han, S.; Tillet, J.; Mulvey, R. Novel Substituted 4-Aminomethylpiperidines as Potent and Selective Human β_3-Agonists. Part 2: Arylethanolaminomethylpiperidines. *Bioorg. Med. Chem. Lett.* **2002**, *12*, 2963–2967. [CrossRef]
5. Malhotra, D.; Page, J.P.; Bowden, M.E.; Karkamkar, A.; Heldebrant, D.J.; Glezakou, V.-A.; Rousseau, R.; Koech, P.K. Phase-Change Aminopyridines as Carbon Dioxide Capture Solvents. *Ind. Eng. Chem. Res.* **2017**, *56*, 7534–7540. [CrossRef]
6. Allen, F.H. The Cambridge Structural Database: A Quarter of a Million Crystal Structures and Rising. *Acta Crystallogr. Sect. B Struct. Sci.* **2002**, *58*, 380–388. [CrossRef]
7. Schutte, M.; Visser, H.G.; Roodt, A. 2-(Ammoniomethyl) pyridinium sulfate monohydrate. *Acta Crystallogr. Sect. E Struct. Rep. Online* **2012**, *68*, o914. [CrossRef]
8. Marouani, H.; Rzaigui, M.; Al-Deyab, S.S. Synthesis and Crystal Structure of $(3\text{-}NH_3CH_2C_5H_4NH)SO_4{\cdot}H_2O$. *X Ray Struct. Anal. Online* **2011**, *27*, 25–26. [CrossRef]
9. Junk, P.C.; Kim, Y.; Skelton, B.W.; White, A.H. The Structural Systematics of Protonation of Some Important Nitrogen-Base Ligands. V. Some Univalent Anion Salts of Mono- and Bis(2-picolyl)amine. *Z. Anorg. Allg. Chem.* **2006**, *632*, 1340–1350. [CrossRef]
10. Liang, W.-X.; Wang, G.; Qu, Z.-R. Redetermination of 3-(ammoniomethyl) pyridinium dichloride. *Acta Crystallogr. Sect. E Struct. Rep. Online* **2009**, *65*, o1814. [CrossRef]
11. de Vries, E.J.C.; Oliver, C.L.; Lloyd, G.O. (4-Pyridylmethyl) aminium chloride. *Acta Crystallogr. Sect. E Struct. Rep. Online* **2005**, *61*, o1577–o1578. [CrossRef]
12. El Glaoui, M.; Kefi, R.; Amri, O.; Jeanneau, E.; Ben Nasr, C. 4-(Ammoniomethyl) pyridinium dichloride. *Acta Crystallogr. Sect. E Struct. Rep. Online* **2008**, *64*, o2204. [CrossRef] [PubMed]
13. Gan, X.; Tang, Z.; Wang, Y.; Zhang, W.; Sun, X.; Wu, Y.; Gao, Z.; Cai, H.-L.; Wu, X.S. Molecular Ferroelectric Piperidine-4-ylmethanaminium Perchlorate with Superior Switchable Dielectric Properties. *ChemistrySelect* **2019**, *4*, 2903–2907. [CrossRef]
14. Deniau, G.; Moraux, T.; O'Hagan, D.; Slawin, A.M.Z. An efficient synthesis of (*R*)-and (*S*)-2-(aminomethyl)piperidine dihydrochloride. *Tetrahedron Asymmetry* **2008**, *19*, 2330–2333. [CrossRef]
15. David, W.I.F.; Shankland, K.; van de Streek, J.; Pidcock, E.; Motherwell, W.D.S.; Cole, J.C. *DASH*: A program for crystal structure determination from powder diffraction data. *J. Appl. Crystallogr.* **2006**, *39*, 910–915. [CrossRef]
16. CCDC-Opensource/Dash. Available online: https://github.com/ccdc-opensource/dash/releases (accessed on 15 October 2024).
17. David, W.I.F.; Shankland, K. Structure determination from powder diffraction data. *Acta Crystallogr. Sect. A Found. Crystallogr.* **2008**, *64*, 52–64. [CrossRef]
18. Shankland, K.; Spillman, M.J.; Kabova, E.A.; Edgeley, D.S.; Shankland, N. The principles underlying the use of powder diffraction data in solving pharmaceutical crystal structures. *Acta Crystallogr. Sect. C Cryst. Struct. Commun.* **2013**, *69*, 1251–1259. [CrossRef]
19. Kabova, E.A.; Cole, J.C.; Korb, O.; Lopez-Ibáñez, M.; Williams, A.C.; Shankland, K. Improved performance of crystal structure solution from powder diffraction data through parameter tuning of a simulated annealing algorithm. *J. Appl. Crystallogr.* **2017**, *50*, 1411–1420. [CrossRef]
20. Kabova, E.A.; Cole, J.C.; Korb, O.; Williams, A.C.; Shankland, K. Improved crystal structure solution from powder diffraction data by the use of conformational information. *J. Appl. Crystallogr.* **2017**, *50*, 1421–1427. [CrossRef]
21. Kaduk, J.A.; Crowder, C.E.; Zhong, K.; Fawcett, T.G.; Suchomel, M.R. Crystal Structure of Atomoxetine Hydrochloride (Strattera), $C_{17}H_{22}NOCl$. *Powder Diffr.* **2024**, *29*, 269–273. [CrossRef]
22. Kaduk, J.A.; Dosen, A.; Blanton, T.N. Crystal structure of ribociclib hydrogen succinate, $(C_{23}H_{31}N_8O)(HC_4H_4O_4)$. *Powder Diffr.* **2024**, *39*, 1–8. [CrossRef]
23. Florence, A.J.; Shankland, N.; Shankland, K.; David, W.I.F.; Pidcock, E.; Xu, X.; Johnston, A.; Kennedy, A.R.; Cox, P.J.; Evans, J.S.O.; et al. Solving molecular crystal structures from laboratory X-ray powder diffraction data with DASH: The state of the art and challenges. *J. Appl. Crystallogr.* **2005**, *38*, 249–259. [CrossRef]

24. Bánhegyi, D.F.; Madarász, J.; Fogassy, E.; Pálovics, E.; Pokol, G. Crystalline Forms of 4, 4'-Methylenediantipyrine: Crystallographic Unit Cell for the Anhydrous Form, from Laboratory Powder XRD Pattern by DASH Program Package. *Period. Polytech. Chem. Eng.* **2023**, *67*, 557–564. [CrossRef]
25. Boultif, A.; Louër, D. Indexing of powder diffraction patterns for low-symmetry lattices by the successive dichotomy method. *J. Appl. Crystallogr.* **1991**, *24*, 987–993. [CrossRef]
26. Markvardsen, A.J.; David, W.I.F.; Johnson, J.C.; Shankland, K. A probabilistic approach to space-group determination from powder diffraction data. *Acta Crystallogr. Sect. A Found. Crystallogr.* **2001**, *57*, 47–54. [CrossRef]
27. Markvardsen, A.J.; Shankland, K.; David, W.I.F.; Johnson, J.C.; Ibberson, R.M.; Tucker, M.; Nowell, H.; Griffin, T. *ExtSym*: A program to aid space-group determination from powder diffraction data. *J. Appl. Crystallogr.* **2008**, *41*, 1177–1181. [CrossRef]
28. Nakamoto, K. *Infrared and Raman Spectra of Inorganic and Coordination Compounds: Part A: Theory and Applications in Inorganic Chemistry*, 6th ed.; John Wiley & Sons, Inc.: Hoboken, NJ, USA, 2009; p. 194.
29. Le Bail, A. Monte Carlo indexing with McMaille. *Powder Diffr.* **2004**, *19*, 249–254. [CrossRef]
30. Hofmann, D.W.M. Fast estimation of crystal densities. *Acta Crystallogr. Sect. B Struct. Sci.* **2002**, *58*, 489–493. [CrossRef]